Optimal Elasticity of Biological Networks

Henrik Ronellenfitsch[1,2]
[1]Department of Mathematics, Massachusetts Institute of Technology, 77 Massachusetts Ave, Cambridge, Massachusetts 02139, USA
[2]Physics Department, Williams College, 33 Lab Campus Drive, Williamstown, Massachusetts 01267, USA

(Received 4 August 2020; accepted 24 December 2020; published 21 January 2021)

Reinforced elastic sheets surround us in daily life, from concrete shell buildings to biological structures such as the arthropod exoskeleton or the venation network of dicotyledonous plant leaves. Natural structures are often highly optimized through evolution and natural selection, leading to the biologically and practically relevant problem of understanding and applying the principles of their design. Inspired by the hierarchically organized scaffolding networks found in plant leaves, here we model networks of bending beams that capture the discrete and nonuniform nature of natural materials. Using the principle of maximal rigidity under natural resource constraints, we show that optimal discrete beam networks reproduce the structural features of real leaf venation. Thus, in addition to its ability to efficiently transport water and nutrients, the venation network also optimizes leaf rigidity using the same hierarchical reticulated network topology. We study the phase space of optimal mechanical networks, providing concrete guidelines for the construction of elastic structures. We implement these natural design rules by fabricating efficient, biologically inspired metamaterials.

DOI: 10.1103/PhysRevLett.126.038101

Elastic sheets reinforced by beams are pervasive in nature and engineering. From concrete shell buildings [1] to aircraft fuselages [2], reinforced shells have found numerous applications due to their rigidity and efficient use of resources. Evolution and natural selection have also produced sheet structures such as plant leaves, which need to remain flat to maximize photosynthesis [3–6], or dragonfly wings, which combine light weight and rigidity to enable efficient flight [7]. Uncovering the design rules behind biologically optimized natural materials may not just impact engineering but also illuminate their role in evolution.

Efficient design of thin shells is an active research problem [8–14], and mechanical metamaterials have emerged as promising candidates for efficient, rigid, and tunable structures [15–20]. Natural materials are often characterized by a fractal-like hierarchical organization. Specifically, the venation of plant leaves is known to play a crucial role in the transport of water and nutrients [21], and in the structural rigidity of the lamina [3,5,6], so as to allow the plant to maximize area for photosynthesis while being compliant with the wind and other forces [22,23]. While much work has been done to characterize the venation networks of dicotyledonous plants in terms of geometry [24–26], topology [27–29], and optimal fluid transport [30–35], the mechanical purpose, properties, and optimality of the venation network beyond the midrib [3,4,36,37] have received less attention [38]. Recent work points toward the importance of mechanical traits [39]. Here, we ask to which extent leaves and similar natural materials may be mechanically optimized, what rules their natural design underlies, and how these rules can be applied.

To answer these questions, we consider a model of discrete beam networks (DBNs) to capture the properties of natural materials. Specifically, DBNs model bending beams with arbitrary stiffness that are joined to form an elastic network. We apply this generic model to the elasticity of leaf venation. We numerically minimize the mechanical compliance, maximizing overall rigidity under natural loads [12], with a resource constraint to model the cost-efficiency trade-off that these networks are subject to [25,34,40–43]. We find that optimized mechanical DBNs exhibit similar structural features as real leaves: a central midrib and hierarchically branching higher order veins connected by anastomoses, in close correspondence to vascular networks found by optimizing for robust liquid transport [21,30–34,44–46]. Features of the leaf venation such as the structure of interconnecting anastomoses and loops are thus naturally explained by mechanical optimization. We identify distinct topological phases as design rules of optimal DBNs that lead to substantially improved rigidity of the network and use these rules to design and manufacture efficient elastic metamaterials.

The theory of elastic sheets connects curvature to an elastic energy [47,48] and has been used with great success to model uniform membranes and shells [49–55]. Methods like topology optimization [12] are tailored for nonuniform continua, and progress has been made optimizing reinforced elastic shells [8,9]. We now consider a simple model of beam networks that captures the discreteness and nonuniformity of

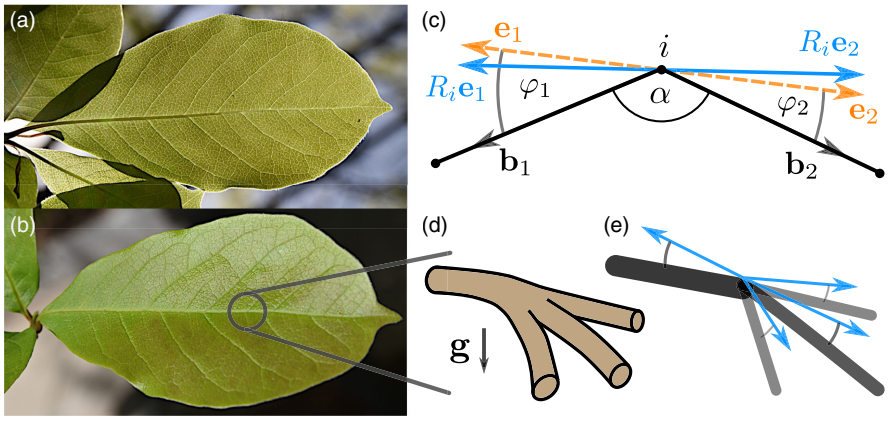

FIG. 1. Leaf venation as a discrete beam network. (a) Abaxial surface of a leaf of *Magnolia sp.*, showing the hierarchically organized reticulate venation network keeping the lamina flat and rigid, and transporting water and nutrients. (b) Adaxial surface of the same leaf, emphasizing the venation network embedded in the lamina. (c) Discrete model of beam bending. Dashed orange arrows correspond to the local reference frame $\{\mathbf{e}_{1,2}\}$ used to construct the elastic energy Eq. (2) with $\sin^2\varphi_{1,2} = \|\mathbf{e}_{1,2}\times\mathbf{b}_{1,2}\|^2$. The reference frame $\{R_i\mathbf{e}_{1,2}\}$ compensating overall rigid rotations is shown in blue. (d) Plant leaf venation subject to gravitational load $\mathbf{g}$ as prototypical example of a natural DBN. One large vein branches off into three smaller veins that all bend under the load. (e) DBN model of the node from (d). Each discrete beam joining at the node is depicted with its bending constant by line thickness and color. Deviations from the local reference (blue) are penalized by Eq. (3).

natural materials. As an illustrative example, take a uniform cylindrical beam with bending energy [56,57],

$$V_b = \frac{\pi}{8} Y \ell r^4 \frac{1}{\mathcal{R}^2} \approx \frac{1}{2}\kappa \sin^2\alpha = \frac{1}{2}\kappa\|\mathbf{b}_1\times\mathbf{b}_2\|^2, \quad (1)$$

where Y is the beam's Young's modulus, r is its radius, ℓ is its length, and $\mathcal{R}$ is its radius of curvature. The bending angle α was introduced by discretizing the beam using the unit vectors $\mathbf{b}_{1,2}$ and approximating the curvature [Fig. 1(c), Ref. [58]]. The constants of proportionality were combined into the bending constant $\kappa = \pi Y r^4/\ell$. It is possible to find an equivalent formulation of Eq. (1) using two elastically connected rigid beams.

We introduce a set of unit vectors $\{\mathbf{e}_1, \mathbf{e}_2\}$ at the midpoint, corresponding to the reference configuration of the beams [Fig. 1(c)]. An elastic energy penalizing deviations from this reference is then

$$V = \frac{1}{2}\kappa_b\|(R\mathbf{e}_1)\times\mathbf{b}_1\|^2 + \frac{1}{2}\kappa_b\|(R\mathbf{e}_2)\times\mathbf{b}_2\|^2, \quad (2)$$

where R is a rotation matrix. This two-beam energy is equivalent to Eq. (1) if R is chosen to compensate any overall rigid rotations, which can be achieved by minimizing V over R at fixed $\mathbf{b}$ [58]. Equation (2) then suggests that the elastic energy of an arbitrary number of beams elastically connected at a node i [Fig. 1(e)] can be written as

$$V_i = \frac{1}{2}\sum_{b\in B_i}\kappa_b\|(R_i\mathbf{e}_b)\times\mathbf{b}\|^2, \quad (3)$$

where the sum runs over the set B_i of edges joining at node i, κ_b is the bending constant of edge b, and $\mathbf{b}$ is the unit vector pointing from node i to node j along the edge $b = (ij)$. The node's equilibrium configuration is given by the local reference frame $\{\mathbf{e}_b\}_{b\in B_i}$ and R_i compensates overall rigid rotations. We now linearize Eq. (3) by expanding both R_i and $\mathbf{b}$ and minimizing over R_i [58]. We find for a network consisting of N nodes,

$$V = \frac{1}{2}\mathbf{u}^\top(H_{\rm eq} - H_{\rm or})\mathbf{u} = \frac{1}{2}\mathbf{u}^\top H\mathbf{u}, \quad (4)$$

where $\mathbf{u}$ is the $3N$-dimensional vector of nodal displacements from equilibrium. The term $(1/2)\mathbf{u}^\top H_{\rm eq}\mathbf{u}$ is the elastic energy with respect to the fixed equilibrium frame $\{\mathbf{e}_b\}$, while $(1/2)\mathbf{u}^\top H_{\rm or}\mathbf{u}$ corrects for overall rotations [58]. Given any static loads $\mathbf{f}$ on the network, the displacements satisfy $H\mathbf{u} = \mathbf{f}$. At each node, this force balance can be expressed as $\mathbf{f}_i = \sum_j(\mathbf{F}_{ij} - \mathbf{F}_{ji})$, where $\mathbf{F}_{ij}$ is the force on node i due to the connection to node j, and $\mathbf{f}_i$ is the load on node i [58].

While our model applies to generic elastic networks, we now specialize to leaflike structures. We consider planar DBNs described by Eq. (4) and embedded in an inextensible lamina. Inextensibility of both beam network and lamina is implemented to linear order by allowing only nodal displacements $\mathbf{u}$ that satisfy $\mathbf{e}_b^\top(\mathbf{u}_j - \mathbf{u}_i) = 0$ for all edges b [51,55,58].

Leaves must remain flat and rigid to present a maximal area to sunlight for photosynthesis. Thus, we expect the reinforced scaffolding network to be optimized under the influence of gravitational or wind load. Maximum rigidity of a mechanical system under loads $\mathbf{f}$ leading to displacements $\mathbf{u}$ corresponds to minimum compliance $c = \mathbf{f}^\top\mathbf{u} = \sum_i \mathbf{f}_i^\top\mathbf{u}_i$ [12], where $\mathbf{f}_i$ is the load on node i and $\mathbf{u}_i$ is its

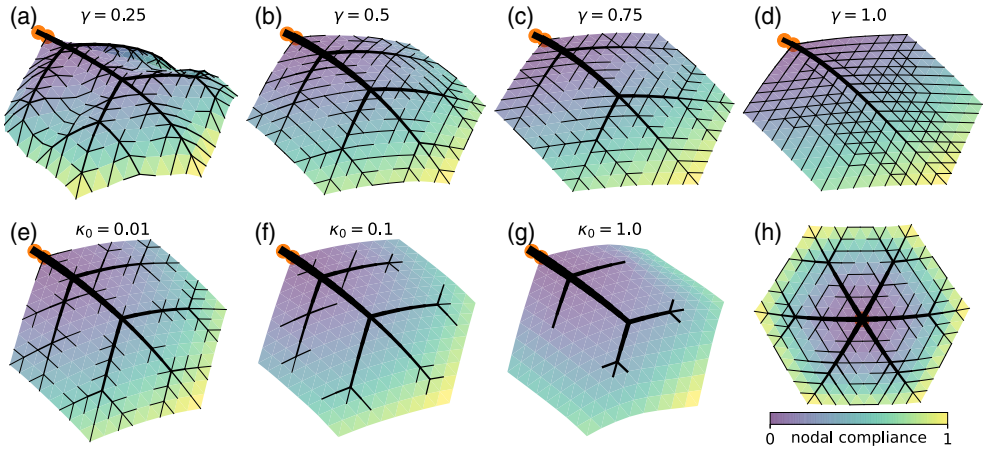

FIG. 2. Compliance-optimized flat DBNs resemble real leaf venation. We optimized triangular DBNs with $N = 217$ nodes and $E_{\text{triang}} = 600$ edges. (a)–(c) For $0 < \gamma < 1$, optimal networks are sparse and show hierarchical organization and anastomosing reticulation. (d) At the transition $\gamma = 1$, the network becomes highly reticulate and less hierarchically organized. The networks (a)–(d) were subject to a uniform downward load, the petiole was modeled as one additional node the position of which was fixed, and overall twists of the petiole were removed. The lamina stiffness was $\kappa_0 = 10^{-6}$. (e)–(g) Optimal networks reduce to just the main veins as the lamina stiffness κ_0 is increased. (h) An optimal network with the petiole at the center and subject to a uniform upward load. The cost parameter in (e)–(h) was $\gamma = 1/2$, and the lamina stiffness in (h) was $\kappa_0 = 10^{-6}$. Fixed nodes are shown as red dots, each triangle is colored by the average nodal compliance $\mathbf{f}_i^\top \mathbf{u}_i$ of the adjacent nodes normalized by the maximum, and the line thicknesses are proportional to $\kappa_b^{\gamma/2}$.

displacement. In the following, we minimize the compliance over the set of bending constants κ_b of the network. Biological networks are constrained by the amount of resources available and by the requirement to distribute them efficiently. Following Refs. [30–33,40,41], we incorporate this by introducing the constraint $\sum_b \kappa_b^\gamma = K$, where the parameter γ models the material cost of each beam and K is the overall cost. A natural material constraint is the total mass of the network, which for beams following Eq. (1) corresponds to $\gamma = 1/2$. More generally, $0 < \gamma < 1$ leads to an economy of scale promoting sparse networks [62]. We now focus on this biologically relevant regime.

The optimal κ_b are encoded in a scaling relation with the nodal forces [58],

$$\kappa_b \sim (\ell_b^2(\|\mathbf{F}_{ij}\|^2 + \|\mathbf{F}_{ji}\|^2))^{1/(1+\gamma)}, \tag{5}$$

where the edge b connects nodes i and j. To avoid local minima due to the nonconvex constraint, we employ a numerical optimization algorithm based on simulated annealing [58]. In the following, we start from a triangular grid in the x-y plane representing the leaf lamina, which is attached to a petiole with fixed position and orientation (Fig. 2, Ref. [58]). The entire leaf is subject to uniform load in the negative z direction [Figs. 1(d) and 1(e)], such that the compliance is now proportional to the average displacement. This is a reasonable approximation given typical leaf mass composition [63]. Including vein self-loads in this regime does not lead to markedly different optimal networks [58]. Because the leaf lamina itself is rigid, we set the bending constants to $\kappa_0 + \kappa_b$, where κ_0 is the lamina stiffness and the κ_b are the bending constants of the network that we minimize over. The inextensibility constraint is enforced on all edges of the triangular grid irrespective of their bending rigidity, such that the lamina is always inextensible to linear order. The cost K is fixed to the number of edges in the triangular grid, setting the scale for the κ_b. We first specialize to the regime $\kappa_0 = 10^{-6} \ll \kappa_b$ where the elastic properties are dominated by the venation network. Here, optimized DBNs are rigid and flat, decreasing the compliance by a factor of $\sim$100 compared to uniform networks [Fig. 3(c)]. Their structure exhibits the basic features of dicotyledonous leaf venation [Figs. 2(a)–2(d)], including a hierarchical midrib and branching and anastomosing higher order veins. This is also reflected in quantitative topological measures when comparing to real leaf networks [58]. Mechanically optimized DBNs are structurally similar to distribution networks optimizing robust fluid transport [30–34]. This is due to a connection between hydraulic and elastic leaf network models, both of which can be seen as conservation laws (of fluid or force) with a single source and many sinks. Furthermore, under the inextensibility constraint, $(1/2)\mathbf{u}^\top H_{\text{eq}}\mathbf{u} = \sum_{i,j}(\kappa_b/\ell_b^2)(u_{z,j} - u_{z,i})^2$, where $u_{z,i}$ are the z components of the displacements [58]. Formally identifying κ_b/ℓ_b^2 with the hydraulic conductivity and the perpendicular displacements $u_{z,i}$ with the potential, this part of the compliance has the same form as the power dissipation minimized for flow networks and encodes only the weighted network topology. Optimal flow networks are

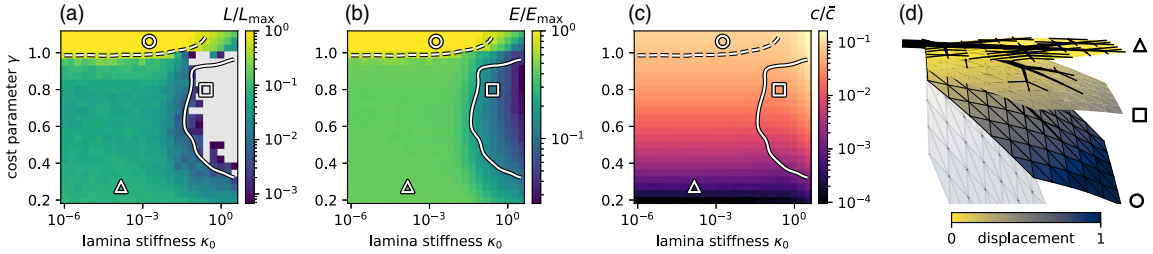

FIG. 3. Topological transition and phase space of optimal DBNs with leaf boundary conditions. Each pixel in the 25×25 images (a)–(c) corresponds to a mean over 10 annealed triangular networks with $N = 92$ nodes and $E_{max} = 241$ edges. (a) Network topology is encoded in the loop density L/L_{max}, where L is the number of loops and $L_{max} = 150$ is the maximum number of loops in the triangular grid. Gray pixels correspond to $L = 0$. The dashed and solid lines approximately mark the transitions to maximally loopy and tree topologies, respectively. (b) Network structure as measured by the number of nonzero bending constant edges E normalized by the maximum number E_{max} of edges in the triangular grid. (c) The compliance c of the optimized networks, normalized by the compliance $\bar{c}$ of a uniform network with identical cost K. The results in (a)–(c) remain qualitatively valid for larger networks [58]. (d) Optimal networks △, □, ◯, and a uniform network shown with their relative displacements under the same load. The optimal networks are also marked in panels (a)–(c). Displacements are measured relative to the tip of network ◯.

known to correspond to topological trees [64], even though the global optimum may not be hierarchical [65]. Thus, the geometric term $\mathbf{u}^\top H_{or}\mathbf{u}$ is responsible for departure from the tree optima and induces redundant connections in mechanical networks [58]. This intrinsic elastic mechanism stands in contrast to flow networks where only explicitly modeling additional effects such as resistance to fluctuations or damage can induce loops [31,32,49]. When $\gamma > 1$, the optimization problem becomes convex, and a single global minimum exists, containing a midrib but otherwise appearing featureless [Fig. 2(d)]. The generic properties of optimal DBNs remain valid for other boundary conditions as well [Fig. 2(h)].

We now proceed to study the topological transition from nonreticulate to reticulate optimal networks. The topology of planar networks is quantified by the number of loops $L = E - N + 1$, as obtained from Euler's formula. Optimal DBNs exhibit three basic topological phases [Fig. 3(a)]. In the convex regime where $\gamma > 1$ and the lamina stiffness $\kappa_0 \lesssim 10^{-2}$, the optimal networks corresponding to the single global minimum are maximally loopy. As γ is decreased below 1, most loops are lost and the optimal networks feature a small number of loops that is approximately constant over a wide range of parameter values. Increasing the lamina stiffness beyond $\kappa_0 \approx 10^{-2}$ leads to a gradual crossover into a loop-less regime, where only main and secondary veins are reinforced [Figs. 2(e)–2(g)]. These transitions are mirrored in the number of nonzero bending constant edges E in the network, with the difference that E gradually decreases as κ_0 is increased instead of dropping to zero [Fig. 3(b)]. Surprisingly, the optimal compliance does not vary strongly with the optimal network topology [Figs. 3(c)]. Instead, the optimal compliance is largely independent of the lamina stiffness κ_0 and varies strongly only with the cost parameter γ. Because γ is expected to be fixed by geometry, this suggests that generically, it pays to invest in an optimized mechanical network, even if this means only reinforcing the main vein. Even then, the improvement in compliance is significant [Fig. 3(c) and 3(d)].

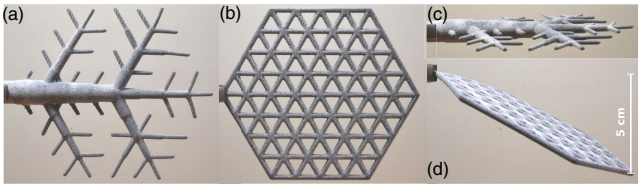

FIG. 4. Biologically inspired metamaterials for flatness and rigidity. (a) Additively manufactured metamaterial based on an optimized DBN topology with $\gamma = 1/2$. The vertical size is 11 cm, the material is thermoplastic polyurethane [58]. (b) Metamaterial based on a uniform DBN topology with equal size and total volume. Beam radii in (a), (b) are proportional to $\kappa_b^{1/4}$, and $\kappa_0 = 0$. (c),(d) Side view of the same networks clamped at the petiole. The optimized network (c) remained flat. The uniform network (d) showed a tip displacement of approximately 5 cm.

The natural design principles of leaf venation can be applied to the design of efficient rigid metamaterials. We additively manufactured networks of connected cylindrical beams based on optimized and uniform DBN topologies with equal material volume [Figs. 4(a) and 4(b), Ref. [58]]. The improvement in rigidity in the optimized manufactured network is significant, with no bending or tip displacement discernible [Fig. 4(c)]. This is compared to the uniform network, which bends visibly [Fig. 4(d)]. This suggests that biologically inspired elastic networks may provide design principles for discrete metamaterials.

In summary, we considered a model of discrete beam networks that is able to naturally represent nonuniform reinforcing scaffoldings of elastic sheets and networks, and applied it to leaf venation. We showed that optimal DBNs minimizing mechanical compliance under a cost constraint resemble real leaves, including a hierarchical backbone,

anastomoses, and loops between the veins. Using the principles learned from nature, we designed and manufactured elastic metamaterials.

Our results may have implications for the biology of leaves and other natural materials with a combined mechanical and hydraulic function such as dragonfly wings [7]. The relevance of fluid flow optimization for leaf venation is well known when rationalizing loops as an evolutionary adaptation to damage or fluctuations [21,34]. At the same time, the reduction in compliance of optimized over uniform DBNs is highly significant. Thus, maximizing stiffness could result in an evolutionary advantage. Leaves are therefore in the extraordinary position to optimize two highly disparate requirements, mechanical rigidity and robust fluid transport, using the same hierarchically organized, reticulate venation network architecture. Our results may also offer a connection between the differing approaches modeling leaf vascular development as adaptive mechanisms relying on either flow [33,66,67] or mechanical [68–72] cues. More generally, our work paves the way for detailed study of optimized mechanical networks in other biological systems such as actin-myosin networks [73], active mechanics [74,75], allosteric materials [76], or network control [77].

The author wishes to thank Ellen A. Donnelly for helpful discussions and the MIT Department of Mathematics for support.

[1] M. Melaragno, *An Introduction to Shell Structures: The Art and Science of Vaulting* (Springer, Boston, MA, 2012).
[2] C. Niu and M. Niu, *Airframe Structural Design: Practical Design Information and Data on Aircraft Structures*, Airframe Book Series (Adaso/Adastra Engineering Center, Granada Hills, 1999).
[3] K. J. Niklas, *Plant Biomechanics: An Engineering Approach to Plant Form and Function* (The University of Chicago Press, Chicago, London, 1992).
[4] K. J. Niklas, A mechanical perspective on foliage leaf form and function, New Phytol. **143**, 19 (1999).
[5] A. Roth-Nebelsick, D. Uhl, V. Mosbrugger, and H. Kerp, Evolution and function of leaf venation architecture: A review, Ann. Botany **87**, 553 (2001).
[6] L. Sack and C. Scoffoni, Leaf venation: Structure, function, development, evolution, ecology and applications in the past, present and future, New Phytol. **198**, 983 (2013).
[7] J. Sun and B. Bhushan, The structure and mechanical properties of dragonfly wings and their role on flyability, C. R. Mécan. **340**, 3 (2012).
[8] F. Gil-Ureta, N. Pietroni, and D. Zorin, Reinforcement of general shell structures, ACM Trans. Graph. **39**, 153 (2020).
[9] Y. Sakai, M. Ohsaki, and S. Adriaenssens, A 3-dimensional elastic beam model for form-finding of bending-active gridshells, Int. J. Solids Struct. **193–194**, 328 (2020).
[10] A. Seranaj, E. Elezi, and A. Seranaj, Structural optimization of reinforced concrete spatial structures with different structural openings and forms, Res. Eng. Struct. Mater. **4**, 79 (2018).
[11] S. Townsend and H. A. Kim, A level set topology optimization method for the buckling of shell structures, Struct. Multidiscip. Optim. **60**, 1783 (2019).
[12] M. P. Bendsøe and O. Sigmund, *Topology Optimization: Theory, Methods, and Applications*, 2nd ed. (Springer, Berlin, Heidelberg, New York, 2003).
[13] E. Ramm, K.-U. Bletzinger, and R. Reitinger, Shape optimization of shell structures, Revue Européenne des Éléments Finis **2**, 377 (1993).
[14] B. Hassani, S. M. Tavakkoli, and H. Ghasemnejad, Simultaneous shape and topology optimization of shell structures, Struct. Multidiscip. Optim. **48**, 221 (2013).
[15] K. Bertoldi, V. Vitelli, J. Christensen, and M. van Hecke, Flexible mechanical metamaterials, Nat. Rev. Mater. **2**, 17066 (2017).
[16] J. T. B. Overvelde, J. C. Weaver, C. Hoberman, and K. Bertoldi, Rational design of reconfigurable prismatic architected materials, Nature (London) **541**, 347 (2017).
[17] A. Gross, P. Pantidis, K. Bertoldi, and S. Gerasimidis, Correlation between topology and elastic properties of imperfect truss-lattice materials, J. Mech. Phys. Solids **124**, 577 (2019).
[18] C. P. Goodrich, A. J. Liu, and S. R. Nagel, The Principle of Independent Bond-Level Response: Tuning by Pruning to Exploit Disorder for Global Behavior, Phys. Rev. Lett. **114**, 225501 (2015).
[19] H. Ronellenfitsch, N. Stoop, J. Yu, A. Forrow, and J. Dunkel, Inverse design of discrete mechanical metamaterials, Phys. Rev. Mater. **3**, 095201 (2019).
[20] G. Gurtner and M. Durand, Stiffest elastic networks, Proc. R. Soc. A **470**, 20130611 (2014).
[21] E. Katifori, The transport network of a leaf, C. R. Phys. **19**, 244 (2018).
[22] A. Ennos, Compliance in plants, in *Compliant Structures in Nature and Engineering*, Vol. 20 (WIT Press, 2005), pp. 21–37.
[23] S. Vogel, *The Life of a Leaf* (University of Chicago Press, Chicago, London, 2012).
[24] I. J. Wright *et al.*, The worldwide leaf economics spectrum, Nature (London) **428**, 821 (2004).
[25] B. Blonder, C. Violle, L. P. Bentley, and B. J. Enquist, Venation networks and the origin of the leaf economics spectrum, Ecol. Lett. **14**, 91 (2011).
[26] U. Kull and A. Herbig, Leaf venation patterns and principles of evolution, in *Evolution of Natural Structures: Proceedings of the 3rd International Symposium of the Sonderforschungsbereich 230*, edited by M. Hilliges (Vorstand des Sonderforschungsbereich 230, 1994 (Natürliche Konstruktionen 9), Stuttgart, 1994), pp. 167–175.
[27] E. Katifori and M. O. Magnasco, Quantifying loopy network architectures, PLoS One **7**, e37994 (2012).
[28] Y. Mileyko, H. Edelsbrunner, C. A. Price, and J. S. Weitz, Hierarchical ordering of reticular networks, PLoS One **7**, e36715 (2012).
[29] H. Ronellenfitsch, J. Lasser, D. C. Daly, and E. Katifori, Topological phenotypes constitute a new dimension in the phenotypic space of leaf venation networks, PLoS Comput. Biol. **11**, e1004680 (2015).

[30] E. Katifori, G. J. Szöllősi, and M. O. Magnasco, Damage and Fluctuations Induce Loops in Optimal Transport Networks, Phys. Rev. Lett. **104**, 048704 (2010).
[31] F. Corson, Fluctuations and Redundancy in Optimal Transport Networks, Phys. Rev. Lett. **104**, 048703 (2010).
[32] D. Hu and D. Cai, Adaptation and Optimization of Biological Transport Networks, Phys. Rev. Lett. **111**, 138701 (2013).
[33] H. Ronellenfitsch and E. Katifori, Global Optimization, Local Adaptation, and the Role of Growth in Distribution Networks, Phys. Rev. Lett. **117**, 138301 (2016).
[34] H. Ronellenfitsch and E. Katifori, Phenotypes of Vascular Flow Networks, Phys. Rev. Lett. **123**, 248101 (2019).
[35] T. Gavrilchenko and E. Katifori, Resilience in hierarchical fluid flow networks, Phys. Rev. E **99**, 012321 (2019).
[36] T. Gilet and L. Bourouiba, Fluid fragmentation shapes rain-induced foliar disease transmission, J. R. Soc. Interface **12**, 20141092 (2015).
[37] Z. Wei, S. Mandre, and L. Mahadevan, The branch with the furthest reach, Europhys. Lett. **97**, 14005 (2012).
[38] Z. Sun, T. Cui, Y. Zhu, W. Zhang, S. Shi, S. Tang, Z. Du, C. Liu, R. Cui, H. Chen, and X. Guo, The mechanical principles behind the golden ratio distribution of veins in plant leaves, Sci. Rep. **8**, 13859 (2018).
[39] B. Blonder, S. Both, M. Jodra, H. Xu, M. Fricker, I. S. Matos, N. Majalap, D. F. Burslem, Y. A. Teh, and Y. Malhi, Linking functional traits to multiscale statistics of leaf venation networks, New Phytol. **228**, 1796 (2020).
[40] S. Bohn and M. O. Magnasco, Structure, Scaling, and Phase Transition in the Optimal Transport Network, Phys. Rev. Lett. **98**, 088702 (2007).
[41] M. Durand, Structure of Optimal Transport Networks Subject to a Global Constraint, Phys. Rev. Lett. **98**, 088701 (2007).
[42] V. M. Savage, L. P. Bentley, B. J. Enquist, J. S. Sperry, D. D. Smith, P. B. Reich, and E. I. von Allmen, Hydraulic trade-offs and space filling enable better predictions of vascular structure and function in plants, Proc. Natl. Acad. Sci. U.S.A. **107**, 22722 (2010).
[43] C. A. Price and J. S. Weitz, Costs and benefits of reticulate leaf venation, BMC Plant Biol. **14**, 234 (2014).
[44] C. D. Murray, The physiological principle of minimum work: I. The vascular system and the cost of blood volume, Proc. Natl. Acad. Sci. U.S.A. **12**, 207 (1926).
[45] G. B. West, J. H. Brown, and B. J. Enquist, A general model for the structure and allometry of plant vascular systems, Nature (London) **400**, 664 (1999).
[46] J. B. Kirkegaard and K. Sneppen, Optimal Transport Flows for Distributed Production Networks, Phys. Rev. Lett. **124**, 208101 (2020).
[47] S. A. Safran, Curvature elasticity of thin films, Adv. Phys. **48**, 395 (1999).
[48] W. Helfrich, Elastic properties of lipid bilayers: Theory and possible experiments, Z. Naturforsch. **28C**, 693 (1973).
[49] E. Katifori, S. Alben, E. Cerda, D. R. Nelson, and J. Dumais, Foldable structures and the natural design of pollen grains, Proc. Natl. Acad. Sci. U.S.A. **107**, 7635 (2010).
[50] E. Couturier, J. Dumais, E. Cerda, and E. Katifori, Folding of an opened spherical shell, Soft Matter **9**, 8359 (2013).
[51] H. S. Seung and D. R. Nelson, Defects in flexible membranes with crystalline order, Phys. Rev. A **38**, 1005 (1988).
[52] H. Liang and L. Mahadevan, The shape of a long leaf, Proc. Natl. Acad. Sci. U.S.A. **106**, 22049 (2009).
[53] A. Guckenberger, M. P. Schraml, P. G. Chen, M. Leonetti, and S. Gekle, On the bending algorithms for soft objects in flows, Comput. Phys. Commun. **207**, 1 (2016).
[54] G. Gompper and D. M. Kroll, Random surface discretizations and the renormalization of the bending rigidity, J. Phys. I **6**, 1305 (1996).
[55] T. A. Witten, Stress focusing in elastic sheets, Rev. Mod. Phys. **79**, 643 (2007).
[56] B. Audoly and Y. Pomeau, in *Elasticity and Geometry* (Oxford University Press, Oxford, 2010), p. 586.
[57] M. Bergou, M. Wardetzky, S. Robinson, B. Audoly, and E. Grinspun, Discrete elastic rods, ACM Trans. Graph. **27**, 1 (2008).
[58] See Supplemental Material at http://link.aps.org/supplemental/10.1103/PhysRevLett.126.038101 for a detailed discussion of the approximations, a derivation the elastic energy and the constrained optimization algorithm, the continuum limit, a discussion of mechanical constraints and optimization under self-loads, three-dimensional DBNs, and a comparison of optimal DBNs to real leaf networks using topological metrics, which includes Refs. [59–61].
[59] M. P. do Carmo, *Differential Geometry of Curves and Surfaces* (Prentice-Hall, London, 1988).
[60] T. C. Lubensky, C. L. Kane, X. Mao, A. Souslov, and K. Sun, Phonons and elasticity in critically coordinated lattices, Rep. Prog. Phys. **78**, 073901 (2015).
[61] M. Bruyneel and P. Duysinx, Note on topology optimization of continuum structures including self-weight, Struct. Multidiscip. Optim. **29**, 245 (2005).
[62] R. Chartrand, Exact reconstruction of sparse signals via nonconvex minimization, IEEE Signal Process. Lett. **14**, 707 (2007).
[63] G. P. John, C. Scoffoni, T. N. Buckley, R. Villar, H. Poorter, and L. Sack, The anatomical and compositional basis of leaf mass per area, Ecol. Lett. **20**, 412 (2017).
[64] J. R. Banavar, F. Colaiori, A. Flammini, A. Maritan, and A. Rinaldo, Topology of the Fittest Transportation Network, Phys. Rev. Lett. **84**, 4745 (2000).
[65] S. Yan, F. Wang, and O. Sigmund, On the non-optimality of tree structures for heat conduction, Int. J. Heat Mass Transfer **122**, 660 (2018).
[66] A. Runions, R. S. Smith, and P. Prusinkiewicz, Computational models of auxin-driven development, in *Auxin and Its Role in Plant Development* (Springer-Verlag, Wien, 2014), pp. 315–357.
[67] P. Dimitrov and S. W. Zucker, A constant production hypothesis guides leaf venation patterning, Proc. Natl. Acad. Sci. U.S.A. **103**, 9363 (2006).
[68] F. Corson, H. Henry, and M. Adda-Bedia, A model for hierarchical patterns under mechanical stresses, Philos. Mag. **90**, 357 (2010).
[69] F. Corson, M. Adda-Bedia, and A. Boudaoud, In silico leaf venation networks: Growth and reorganization driven by mechanical forces, J. Theor. Biol. **259**, 440 (2009).

[70] M. F. Laguna, S. Bohn, and E. A. Jagla, The Role of Elastic Stresses on Leaf Venation Morphogenesis, PLoS Comput. Biol. **4**, e1000055 (2008).

[71] Y. Bar-Sinai, J.-D. Julien, E. Sharon, S. Armon, N. Nakayama, M. Adda-Bedia, and A. Boudaoud, Mechanical Stress Induces Remodeling of Vascular Networks in Growing Leaves, PLoS Comput. Biol. **12**, e1004819 (2016).

[72] Y. Couder, L. Pauchard, C. Allain, M. Adda-Bedia, and S. Douady, The leaf venation as formed in a tensorial field, Eur. Phys. J. B **28**, 135 (2002).

[73] D. Mizuno, C. Tardin, C. F. Schmidt, and F. C. MacKintosh, Nonequilibrium mechanics of active cytoskeletal networks, Science **315**, 370 (2007).

[74] P. Ronceray, C. P. Broedersz, and M. Lenz, Fiber networks amplify active stress, Proc. Natl. Acad. Sci. U.S.A. **113**, 2827 (2016).

[75] N. Noll, M. Mani, I. Heemskerk, S. J. Streichan, and B. I. Shraiman, Active tension network model suggests an exotic mechanical state realized in epithelial tissues, Nat. Phys. **13**, 1221 (2017).

[76] J. W. Rocks, N. Pashine, I. Bischofberger, C. P. Goodrich, A. J. Liu, and S. R. Nagel, Designing allostery-inspired response in mechanical networks, Proc. Natl. Acad. Sci. U.S.A. **114**, 2520 (2017).

[77] J. Z. Kim, Z. Lu, S. H. Strogatz, and D. S. Bassett, Conformational control of mechanical networks, Nat. Phys. **15**, 714 (2019).